CHEMBIOCHEM

ChemPubSoc Europe

DOI: 10.1002/cbic.201200629

Can Phosphate-Branched RNA Persist under Physiological Conditions?

Tuomas A. Lönnberg*[a]

A 2′-*O*-methyl-RNA oligonucleotide containing a single free 2′-OH group flanking a branching phosphotriester linkage was prepared as a model for phosphate-branched RNA by using an orthogonally protected dimeric phosphoramidite building block in solid-phase synthesis. The strategy allows the synthesis of phosphate-branched oligonucleotides, the three branches of which may be of any desired sequence. Hydrolytic reactions of the phosphotriester linkages in such oligonucleotides were studied at physiological pH in the presence (and absence) of various complementary oligonucleotides. The fully hybridized oligonucleotide model is an order of magnitude more stable than its single-stranded counterpart, which, in turn, is an order of magnitude more stable than its trinucleoside phosphotriester core lacking any oligonucleotide arms. Furthermore, kinked structures obtained by hybridizing the phosphate-branched oligonucleotide with partially complementary oligonucleotides are three to five times more stable than fully double-stranded ones and only approximately three times less stable than the so-called RNA X structure, which has been postulated to incorporate an RNA phosphotriester linkage. The results indicate that when the intrinsically unstable RNA phosphotriester linkage is embedded in an oligonucleotide of appropriate tertiary structure, its half-life can be at least several hours.

Introduction

Branched nucleic acids have been shown to be biologically relevant species—lariat RNA, with oligonucleotide chains extending from all the three sugar hydroxy groups, for example, is a stable and well-established product of the splicing of eukaryotic pre-mRNA.[1] In principle, another mode of branching, through a phosphotriester linkage, would also be available to nucleic acids. In the case of RNA, such a linkage would be inherently unstable owing to facile intramolecular attack of the neighboring 2′-OH group on the neutral phosphate;[2,3] the half-life of the trinucleoside-3′,3′,5′-monophosphate **1** (Scheme 1 A) at 25 °C and pH 7.4, for example, is only approximately 3 min.[4]

An RNA phosphotriester linkage embedded within an oligonucleotide structure can, however, be substantially more stable,[5] even if the oligonucleotide does not form a well-defined structure such as a double helix (Scheme 1 B, compound **2**).[6] In fact, such a structure, the so-called RNA X (Scheme 1 C), has been reported as a product of a model reaction of eukaryotic splicing. Whereas in the presence of all the critical components of the spliceosome—that is, two of the spliceosomal RNAs and two substrate RNAs resembling the 5′-splice site and the branch site—a reaction mimicking the first step of splicing takes place,[7] in the absence of the 5′-splice site mimic the branch site nucleoside instead attacks one of the spliceosomal RNAs, resulting in an anomalous X-shaped oligonucleotide product, the so-called RNA X.[8,9] On the basis of the iodoethanol cleavage patterns of phosphorothioate-substituted RNA X and the susceptibility of RNA X to alkaline hydrolysis, it was proposed that the two oligonucleotide strands could be connected through a trinucleoside phosphotriester linkage.

In the proposed RNA X structure, the phosphotriester linkage is part of an unusual structural motif, connecting two double-helical stems of a four-way junction.[8,9] A structure of

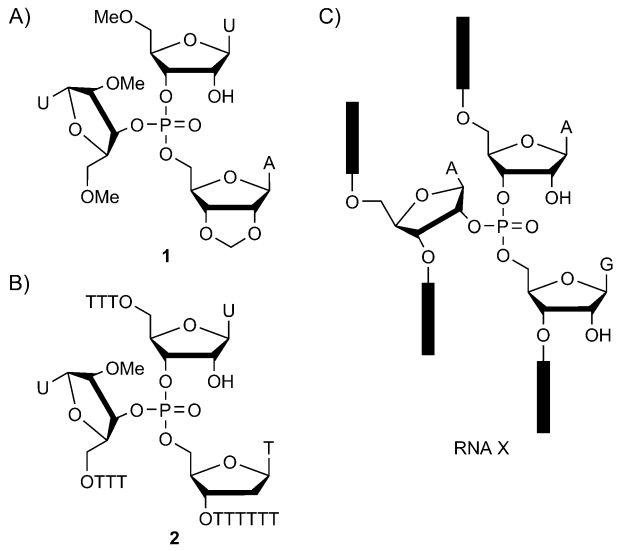

Scheme 1. A) Trinucleoside-3′,3′,5′-monophosphate model compound **1**, B) short phosphate-branched oligonucleotide model compound **2**, and C) the proposed trinucleoside phosphotriester linkage in RNA X.

[a] *Dr. T. A. Lönnberg*
Department of Chemistry, University of Turku
Vatselankatu 2, 20014 Turku (Finland)
E-mail: tuanlo@utu.fi

Supporting information for this article is available on the WWW under http://dx.doi.org/10.1002/cbic.201200629.

this kind could provide some additional stabilization by retarding the formation or the pseudorotation of the pentacoordinate phosphorane intermediate or by shielding the reaction center from solvent. The reported half-life for the decomposition of RNA X at 50 °C and pH 9.0 is approximately 20 min, almost 3000 times longer than extrapolation from the data obtained for **1** would predict.[4,9]

To study the impact of various structural motifs on the hydrolytic stability of an RNA phosphotriester linkage, a phosphate-branched 2′-*O*-methyl-RNA oligonucleotide incorporating a single 2′-OH function protected with a removable protecting group (one flanking the scissile phosphotriester linkage) was synthesized and its hydrolytic reactions were followed at physiological pH in the presence and in the absence of a number of (partly) complementary oligonucleotides. Because the reactive component of the model system is the same in all cases, any changes in the reactivity should be due either to increased entropic penalty for cleaving an internucleosidic bond within a hybridized oligonucleotide or to changes in the geometry or solvation of the active site.

Results

Preparation of the branching phosphoramidite building block

As previously described for symmetric phosphate-branched oligonucleotides, incorporation of the branching trinucleoside phosphotriester linkage is conveniently achieved by coupling of a dimeric phosphoramidite building block to the 5′-OH group of a CPG-supported oligonucleotide.[10] In the present case, however, the requirement for all of the oligonucleotide branches to have unique sequences and the need for removable 2′-protection of one of the nucleosides flanking the phosphotriester linkage present additional synthetic challenges. The 5′-OH groups of the two nucleosides have to be protected by orthogonal protecting groups removable under conditions under which the linker and the nucleobase protecting groups are stable. Furthermore, the protection of the 2′-OH group of one of the nucleosides must be not only orthogonal to both of the 5′-protecting groups but also rapidly removable because of the (presumed) high reactivity of the product. For the 5′-protecting groups, 4,4′-dimethoxytrityl and levulinoyl groups were chosen, whereas the 2′-position was protected with a *tert*-butyldithiomethyl group, removable under reducing conditions.[11]

The preparation of the branching phosphoramidite building block is shown in Scheme 2. Firstly, both of the free hydroxy functions of 2′-*O*-methyluridine were protected as *tert*-butyldimethylsilyl ethers. The 5′-protecting group was then selectively removed under acidic conditions and the free 5′-OH group was protected as a levulinoyl ester. Finally, the 3′-protecting group was removed by conventional fluoride treatment, the free 3′-OH group was phosphitylated with *N*,*N*,*N*′,*N*′-tetraisopropylchlorophosphorodiamidite, and the obtained phosphorodiamidite **7** was coupled with ′-*O*-(*tert*-butyldithiomethyl)-5′-*O*-(4,4′-dimethoxytrityl)uridine, prepared as described previously.[11] During coupling in acetonitrile, decomposition of the product to phosphorothioate-type side products, as reported by Semenyuk et al.,[11] was observed but with use of the highly efficient 5-benzylthio-1*H*-tetrazole as an activator, the coupling could be performed in a short enough time to minimize this side reaction. In the absence of acetonitrile, the final product **8a** proved stable enough to be purified by silica gel chromatography and stored for several months at −20 °C.

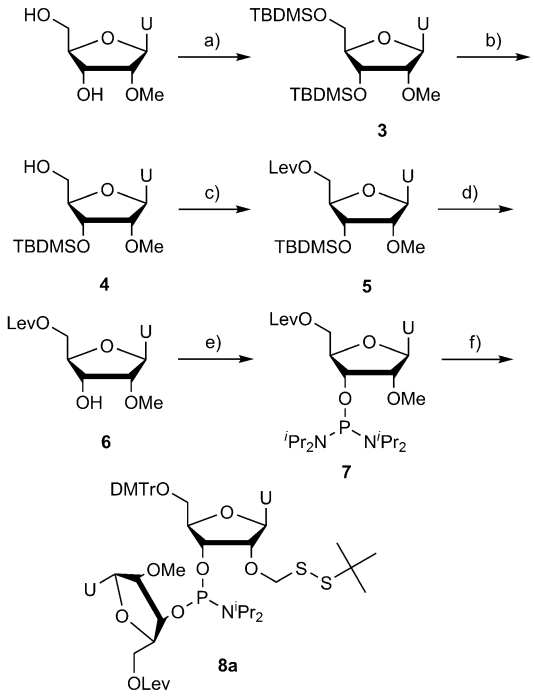

Scheme 2. Preparation of the branching phosphoramidite building block **8a**. a) TBDMSCl, imidazole, DMF; b) TFA, H_2O, THF; c) Lev_2O, pyridine; d) $Et_3N{\cdot}3HF$, THF; e) *N*,*N*,*N*′,*N*′-tetraisopropylchlorophosphorodiamidite, Et_3N, CH_2Cl_2; f) 2′-*O*-(*tert*-butyldithiomethyl)-5′-*O*-(4,4′-dimethoxytrityl)uridine, 5-benzylthio-1*H*-tetrazole, MeCN.

By a similar approach (Scheme 3), a 2′-*tert*-butyldimethylsilyl-protected version (compound **8b**) of the dimeric phosphoramidite was also prepared, but the TBDMS protection was found to be too stable for the kinetic studies (data not shown). However, this building block was successfully employed for the syn-

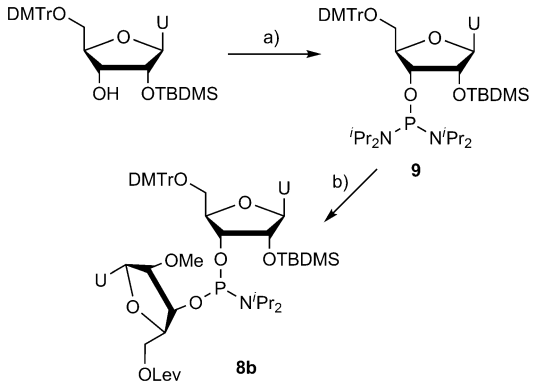

Scheme 3. Preparation of the branching phosphoramidite building block **8b**. a) *N*,*N*,*N*′,*N*′-tetraisopropylchlorophosphorodiamidite, Et_3N, CH_2Cl_2; b) **6**, 5-benzylthio-1*H*-tetrazole, MeCN.

thesis of a reference oligonucleotide incorporating a 3′,3′-phosphodiester linkage.

Oligonucleotide synthesis

The synthesis of the phosphate-branched oligonucleotide **10a** is outlined in Scheme 4. Coupling of the branching phosphoramidite building block **8a** to the 5′-OH group of the CPG-supported oligonucleotide was performed manually with 5-benzylthio-1*H*-tetrazole as the activator. The coupling yield was 54%. The synthesis was then continued on an oligonucleotide synthesizer by using the 5′-DMTr-protected nucleoside as the starting point. The subsequent couplings proceeded with normal efficiency (>99%). For elongation of the branch, the 5′-OH group of the support-bound main-chain oligonucleotide was acetylated and the 5′-levulinoyl protection of the branch site nucleoside was removed with hydrazine acetate. The branch was then synthesized on an oligonucleotide synthesizer and by using the free 5′-OH group as the starting point. To avoid cleavage of the phosphodiester linkage, 40% $MeNH_2$ (90 min at room temperature) was used instead of the conventional aqueous NH_3 treatment for deprotection and release of the oligonucleotide from the support.

For a reference for one of the expected cleavage products, an oligonucleotide incorporating a 3′,3′-phosphodiester linkage (compound **11**, Scheme 5) was synthesized on a CPG-supported 2-(2-hydroxyethylsulfonyl)ethyl succinate linker (a universal linker designed for the synthesis of oligonucleotide-3′-monophosphates)[12] with use of the 2′-*O*-TBDMS-protected branching phosphoramidite **8b** as the first building block. In this case, the coupling efficiency was 80%, with the subsequent couplings proceeding with normal efficiency (>99%). Capping of the first chain and assembly of the second one were then carried out as described above for the branched oligonucleotide **10a**, with similar coupling yields. After deprotection of the nucleobase(s) and release from the support, the 2′-*O*-TBDMS protection was removed with the conventional $Et_3N{\cdot}3HF$ treatment and the product mixture was passed through a short RP cartridge. In both cases, the final oligonucleotide product (**10a** or **11**) was purified by anion-exchange HPLC, followed by desalting by RP HPLC. Attempts to separate the two diastereomers (R_P and S_P) of **10a** were unsuccessful.

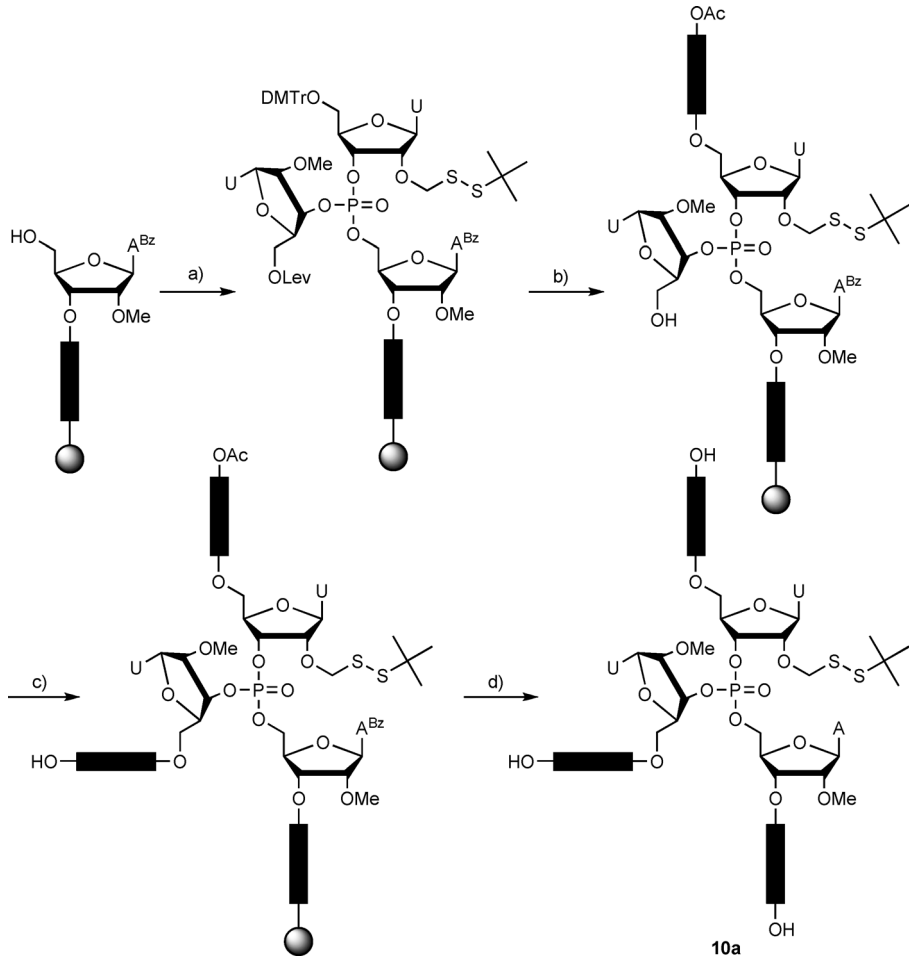

Scheme 4. Preparation of the phosphate-branched oligonucleotide **10a**. a) i: **8a**, 5-benzylthio-1*H*-tetrazole, MeCN, ii: conventional Ac_2O capping, iii: I_2, 2,6-lutidine, H_2O, THF; b) i: conventional phosphoramidite strategy, ii: conventional Ac_2O capping, iii: hydrazine, AcOH, pyridine; c) conventional phosphoramidite strategy; d) $MeNH_2$, H_2O.

Reaction pathways and product distribution

The hydrolysis of the phosphate-branched oligonucleotide **10a** was carried out at 25 °C and pH 7.38 in a 50 mmol L^{-1} tris(2-carboxyethyl)phosphine (TCEP) buffer. Under these reducing conditions, the disulfide bond of the 2′-*O*-*tert*-butyldithiomethyl protecting group is rapidly cleaved, yielding the 2′-thiohemiacetal counterpart **10b** (Scheme 6). The hydrolysis of this intermediate, in turn, releases the desired oligonucleotide model compound **10c** containing a free 2′-OH group flanking the scissile phosphotriester linkage.

The hydroxide-ion-catalyzed cleavage of this phosphotriester was studied by anion-exchange HPLC with the branched oligonucleotide **10c**, either in single-stranded form or hybridized with various partially complementary oligonucleotides (Scheme 7). To minimize the hydrolysis of the starting material during analysis, the HPLC runs were performed at 25 °C, rather than at a higher, denaturing temperature. Whereas the

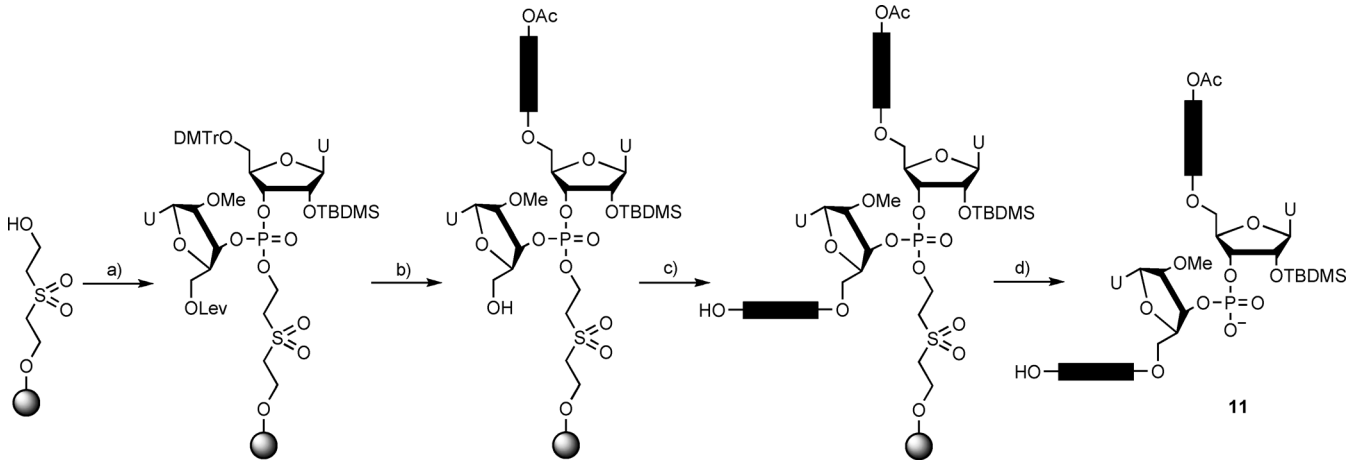

Scheme 5. Preparation of the reference oligonucleotide **11** incorporating a 3′,3′-phosphodiester linkage. Reagents and conditions: a) i: compound **8b**, 5-benzylthio-1*H*-tetrazole, MeCN, ii: conventional Ac_2O capping, iii: I_2, 2,6-lutidine, H_2O, THF; b) i: conventional phosphoramidite strategy, ii: conventional Ac_2O capping, iii: hydrazine, AcOH, pyridine; c) conventional phosphoramidite strategy; d) NH_3, H_2O.

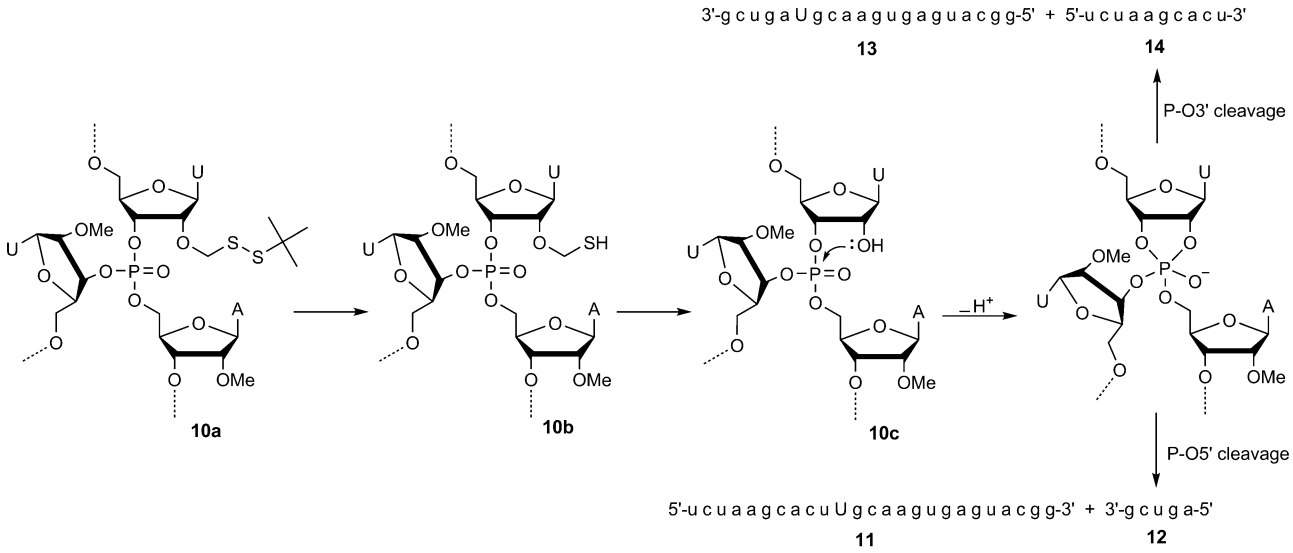

Scheme 6. Hydrolytic reactions of the phosphate-branched oligonucleotide **10a**. In the oligonucleotide products, the lowercase letters refer to 2′-*O*-methylated nucleosides, whereas the uppercase "U" denotes the single nucleoside containing a free 2′-OH in each case.

longer oligonucleotides remained hybridized under these conditions, the shorter products were well resolved, allowing reliable analysis. With the fastest reaction studied (single-stranded **10c**), approximately 25% of the starting material decomposed during a single HPLC run but this loss was uniform for all of the samples, not constituting a major source of inaccuracy. In all the other cases, the decomposition of the starting material during analysis was less than 3%.

From our previous experience with related phosphotriester models, the reaction is first-order in hydroxide ion concentration under the conditions used and proceeds via a monoanionic pentacoordinated phosphorane intermediate (Scheme 6).[2–4,6,13] Unlike the dianionic phosphorane species obtained in the hydroxide-ion-catalyzed cleavage of RNA phosphodiester bonds, this intermediate may pseudorotate to yield both isomerization products and P–O3′ and P–O5′ cleavage products. With all the systems studied, two distinct sets of shorter oligonucleotide products were indeed observed: 25-mer and pentamer oligonucleotides (**11** and **12**, respectively), resulting from the cleavage of the P–O5′ bond of the pentacoordinate phosphorane intermediate, and 20-mer and decamer oligonucleotides (**13** and **14**, respectively) resulting from the cleavage of the P–O3′ bond (Scheme 6). Product distributions for the hydrolysis of **10c** within various oligonucleotide assemblies were determined by comparing the relative concentrations of the pentamer and decamer products **12** and **14**. The results, along with those previously obtained for the corresponding small phosphotriester model compound **1**[4] and the small chimeric phosphate-branched oligonucleotide **2** (Scheme 1),[6] are presented in Table 1.

In contrast to previous results on related systems,[4,6] cleavage of the P–O5′ bond leading to an unnatural 3′,3′-phospho-

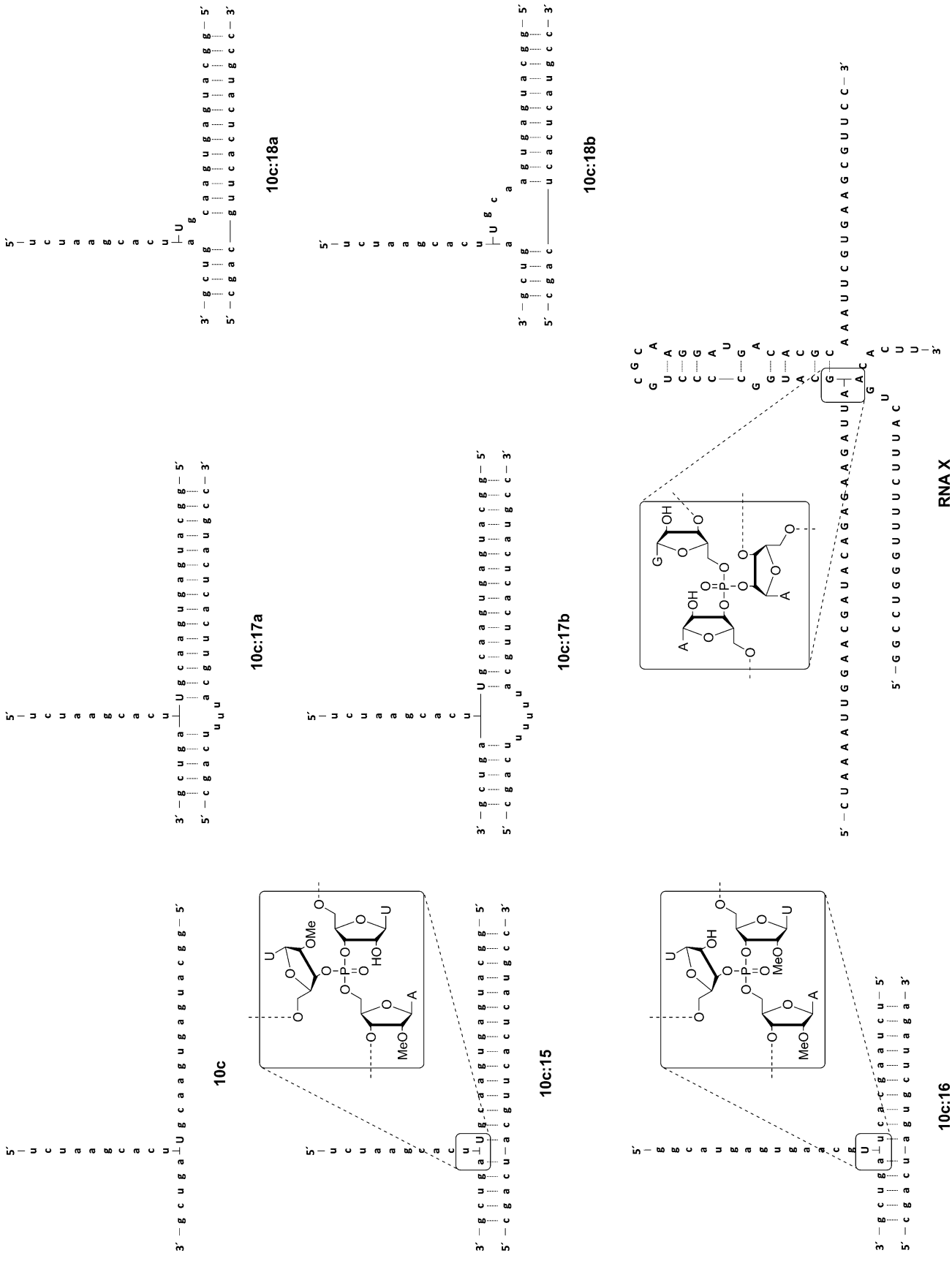

Scheme 7. The oligonucleotide assemblies used in this study, along with the proposed structure of RNA X (adapted from ref. [9]). The lowercase letters refer to 2′-*O*-methylated nucleosides and the uppercase ones to native ribonucleosides.

Table 1. Second-order rate constants and product distributions for the hydroxide-ion-catalyzed cleavage of the phosphotriester linkage of **10c** in the model assemblies of this study [$T = 25\,^{\circ}C$, pH 7.4, $I(NaCl) = 0.22\ mol\,L^{-1}$]. For comparison, corresponding data for the related small phosphotriester model compound **1** and the small chimeric phosphate-branched oligonucleotide **2** (Scheme 1) are also included.

Model	k^{OH} [$L\,mol^{-1}\,s^{-1}$]	% (P–O5′)[a]	% (P–O3′)[b]
1	7500[c]	32[c]	68[c]
2	620[d]	9[d]	8[d]
10c	570 ± 110	63	37
10c:**15**	80 ± 10	80	20
10c:**16**	44 ± 9	n.d.[e]	n.d.[e]
10c:**17a**	18 ± 9	70	30
10c:**17b**	20 ± 4	67	33
10c:**18a**	20 ± 2	69	31
10c:**18b**	31 ± 4	72	28

[a] The ratio of P–O5′ bond fission to overall hydrolysis, determined as the mole fraction of the pentamer oligonucleotide product **12**. [b] The ratio of P–O3′ bond fission to overall hydrolysis, determined as the mole fraction of the decamer oligonucleotide product **14**. [c] From ref. [4]. [d] From ref. [6]. [e] Could not be determined, due to strong association of the decamer product oligonucleotide **14** with the complementary 15-mer oligonucleotide **16**.

diester linkage predominates in all of these model systems. Somewhat unexpectedly, P–O5′ fission is most strongly favored when the main chain of **10c** (containing the sole nucleoside with a free 2′-OH group) is fully hybridized with a complementary oligonucleotide (**10c**:**15**, Figure 1). In contrast, in the cleavage of RNA phosphodiester linkages, P–O5′ fission is retarded by a factor of 15 upon hybridization of the substrate strand.[14] It should be borne in mind, however, that cleavage of ribonucleoside-3′-phosphotriesters proceeds via relatively stable monoanionic phosphorane intermediates that might pseudorotate and, hence, expel any of the alkoxy ligands. The dianionic intermediates of the cleavage of RNA phosphodiester linkages, on the other hand, cannot pseudorotate, making the reaction much more dependent on the ability of the starting material to assume a favorable conformation for direct in-line displacement of the 5′-linked nucleoside. As previously observed for the small model compound **1**,[4] the phosphate-branched oligonucleotide **10c** in all likelihood also undergoes a very rapid isomerization to the 2′,3′,5′ isomer so that the 20-mer and 25-mer oligonucleotide products **13** and **11** are also actually mixtures of two isomers. The mobilities of these oligonucleotides in anion-exchange HPLC were so similar, however, that only a single peak for each of the products was detected. In other words, although both the rate of isomerization and the isomeric ratio probably also reflect changes in the secondary structure of **10c**, no data for this reaction could be obtained.

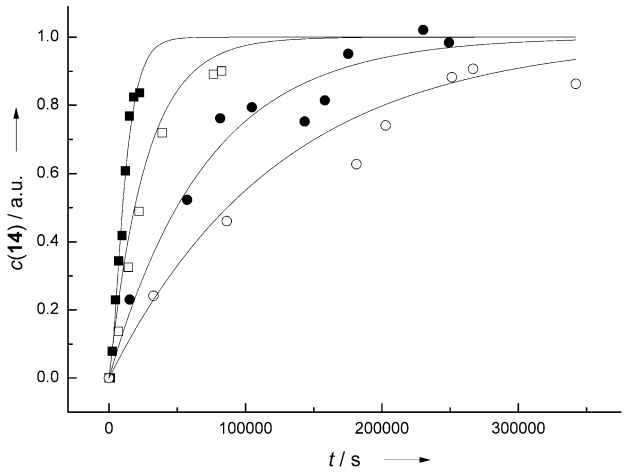

Figure 1. Time-dependent formation of **14** from single-stranded **10c** (■) and from **10c** hybridized with **15** (□), **16** (●), and **17a** (○). $T = 25\,^{\circ}C$, pH 7.38, $I(NaCl) = 0.22\ mol\,L^{-1}$.

Hydrolytic stability of the phosphotriester linkage in various oligonucleotide environments

The rates of cleavage of the phosphate-branched oligonucleotide **10c**, either single-stranded or hybridized with various partly complementary oligonucleotides, at 25 °C and pH 7.38 were determined by monitoring the formation of the decamer oligonucleotide product **14** by anion-exchange HPLC. In all cases, the reactions followed first-order kinetics and the formation of **14** was accompanied by formation of the 20-mer product **13** and the disappearance of **10c**. Illustrative examples of the time-dependent formation of **14** are presented in Figure 1.

As could be expected, the most reactive model system is that consisting only of the single-stranded phosphate-branched oligonucleotide **10c**. The second-order rate constant for the hydroxide-ion-catalyzed cleavage of the phosphotriester linkage is essentially identical to that previously obtained for the related but simpler model compound **2** (Scheme 1) incorporating only uridine and thymidine residues (Table 1). In other words, the (presumably) more extensive base-stacking of **10c** does not confer any additional stabilization relative to its all-pyrimidine counterpart **2**. Both **10c** and **2** are more than an order of magnitude more stable than the small trinucleoside monophosphate **1**, however. In RNA X, the immediate surroundings of the phosphotriester core are even more purine-rich, possibly accounting for some of the greater stability of this species.

Hybridization of the main chain of **10c** with the fully complementary oligonucleotide **15** stabilizes the branching phosphotriester linkage by an order of magnitude but, unexpectedly, cleavage of the P–O5′ bond is not specifically retarded. In fact, the ratio of P–O5′ to P–O3′ fission is somewhat increased on going from the single-stranded **10c** to the double-stranded **10c**:**15** model. The P–O5′ bond is part of the double-helical main chain of the **10c**:**15** assembly, whereas the P–O3′ bond merely connects this double helix to a single-stranded decamer oligonucleotide side arm. Cleavage of the former bond would hence be expected to disrupt the base-stacking within **10c**:**15** much more than cleavage of the latter, yet this is not reflected in the product ratio. When **10c** is hybridized with the shorter oligonucleotide **16**, complementary to the decamer rather than the 15-mer branch, a different model system is obtained. Here the double helix consists solely of 2′-*O*-methylated

nucleosides and the 2′-OH nucleophile is located in the first nucleophile of the single-stranded sidearm. In this model, the phosphotriester linkage is approximately twice as stable as in **10c**:**15**. Unfortunately, because of the tendency of the decamer oligonucleotide product **14** to remain hybridized with **16**, the product ratio for this system could not be determined reliably.

In the proposed structure of RNA X, the putative phosphotriester linkage is not part of a double helix but joins two double-helical stem regions in a four-way junction motif.[8,9] To simulate the effect of such an environment on the stability of an RNA phosphotriester linkage, the hydrolysis of **10c** was studied in the presence of the partially complementary oligonucleotides **17a**, **17b**, **18a**, and **18b**. Hybridization with **17a** or **17b** places the scissile phosphotriester linkage in a kinked position between two double-helical stems, whereas hybridization with **18a** or **18b** results in a bulge containing the phosphotriester within **10c**. Interestingly, in all of these kinked models, the phosphotriester linkage is more stable than those in either of the fully double-helical models **10c**:**15** or **10c**:**16**. The greatest stabilization was observed with **10c**:**17a**, which is hydrolyzed nearly five times more slowly than the fully hybridized **10c**:**15** and more than 400 times more slowly than the corresponding small trinucleoside monophosphate model compound **1**.

The quantitative kinetic data for the decomposition of RNA X were obtained at 50 °C between pH 9 and 12.[9] Extrapolation from these conditions to those used in this study is not a straightforward task, due to the potential for disruption of the secondary structure of RNA at such a high temperature and pH values. If the dependence of rate on temperature is assumed to be similar to that reported for corresponding phosphodiesters,[15] however, a half-life of approximately 2 h would be obtained for RNA X at 25 °C and pH 9. In contrast with simple phosphotriester models,[4,6] the data obtained for RNA X between pH 9 and 12 would suggest a less than first-order dependence of rate on hydroxide ion concentration and possibly even a pH-independent reaction below pH 9.[9] Assuming the reaction to be first-order in [OH^-] hence gives an upper limit of 80 h for the half-life of RNA X at 25 °C and pH 7.4. Although subject to marked uncertainty, this value would indicate that the most stable of the phosphate-branched oligonucleotide models (**10c**:**17a**) is only three times as reactive as RNA X; this would lend further support to the proposal that the two strands of RNA X are connected by a phosphotriester linkage.

Discussion

Perhaps the simplest explanation for the stabilization of a ribonucleotide 3′-phosphotriester by an oligonucleotide environment is that cleavage of the phosphotriester linkage disrupts base stacking of the oligonucleotide chain, leading to an energetically less favorable reaction. If this were the case, however, one would expect the longer phosphate-branched oligonucleotide **10c**, consisting of a mixture of purine and pyrimidine bases, to be hydrolytically more stable than its relatively short homopyrimidine counterpart **2**, whereas in fact these two oligonucleotides react at essentially identical rates. Furthermore, in the fully double-stranded model **10c**:**15**, the P–O5′ bond does not experience greater stabilization than the P–O3′ bond (relative to single-stranded **10c**), even though the former is part of the backbone of a double helix and the latter is not. The greater stabilities of the kinked structures **10c**:**17a**, **10c**:**17b**, **10c**:**18a**, and **10c**:**18b** relative to the fully double-stranded **10c**:**15** are also not easily understood in terms of base stacking alone. Finally, under the conditions used in this study, the phosphodiester linkages of polyuridylic acid are cleaved at the same rate as that of UpU, despite the much more extensive base stacking of the former.[16]

As discussed above, hydroxide-ion-catalyzed cleavage of ribonucleoside 3′-phosphotriesters proceeds via relatively stable monoanionic phosphorane intermediates that may pseudorotate. In other words, in-line arrangements of the nucleophile, the phosphorus atom, and the leaving group in the initial state are not required, unlike in the corresponding reactions of RNA phosphodiester linkages. The formation of the monoanionic phosphorane intermediates might, however, be hindered by unfavorable initial state geometries around the scissile phosphotriester linkages. In particular, an orientation of the phosphorus atom away from the flanking 2′-OH group would be expected to retard the nucleophilic attack yielding this intermediate significantly. Of the model systems studied, the most stable one (**10c**:**17a**) places the scissile phosphotriester linkage in a kinked position against a three-nucleotide bulge, resembling the so-called K-turn motif.[17] In K-turn motifs, the dinucleotide hinges joining the two double-helical regions are characterized by unusually large ε torsion angles of up to 270°.[17,18] For comparison, the corresponding average value for canonical A-type RNA is 210°. An ε angle of 270° translates into nearly the maximum possible distance between the phosphorus atom of the scissile phosphotriester linkage and the 2′-OH nucleophile (Figure 2), and this offers a possible explanation for the observed stabilization, at least in the case of model **10c**:**17a** (and possibly also **10c**:**17b**). It should be noted that the branched oligonucleotide **10c** used was a mixture of R_P and S_P diastereomers and, in all likelihood, of 3′,3′,5′- and 2′,3′,5′-isomers, all of which could react at different rates, especially when hybridized with another oligonucleotide. Furthermore, in RNA X the branching oligonucleotide is connected through a 2′-OH group located in the middle of the strand, rather than a terminal 3′-OH (as is the case with **10c**). Clearly,

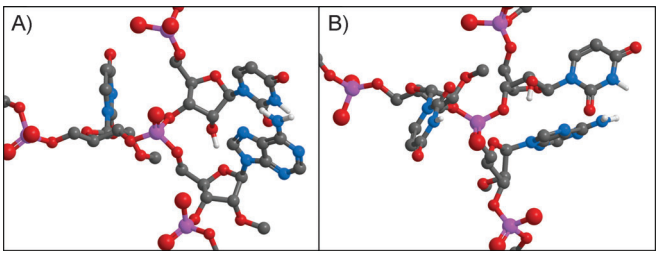

Figure 2. The phosphotriester branch of **10c**: A) in the canonical A-type conformation, and B) as part of a K-turn structural motif. In each case only the S_P diastereomer is shown.

care should be exercised when interpreting these results in terms of the stability of RNA X. We would like to suggest, however, that the extra bulk of the fourth oligonucleotide strand could well serve to hold the phosphotriester linkage away from the 2′-OH nucleophile, resulting in additional stabilization relative to **10c**.

The original RNA X structure was only obtained in the presence of Mg^{2+} (or, to a lesser extent, Ca^{2+}).[8,9] Undoubtedly, the catalytically important metal ions interact closely with the components forming the unusual phosphotriester structure and are very likely coordinated to the branching phosphate itself, as well as the flanking 2′-OH group. Such coordination has been directly observed in the case of group II introns[19] and has also been proposed, on the basis of thio effects, in the case of the spliceosome.[20] Both of these structures promote splicing reactions, in which external nucleophiles are able to outcompete the neighboring 2′-OH groups in attacking the phosphorus atoms of scissile phosphodiester linkages.[21] It seems likely that the metal ions at the reaction centers play a role in preventing nucleophilic attack by the flanking 2′-OH groups either by orienting them away from the scissile phosphate groups or by reducing their nucleophilicities. Such contributions by the Mg^{2+} or Ca^{2+} ions mandatory for the formation of RNA X might explain the somewhat higher stability of this unusual species relative to the phosphate-branched models presented in this paper.

Conclusions

An orthogonally protected dimeric phosphoramidite building block for the synthesis of phosphate-branched oligonucleotides of arbitrary sequence has been prepared and employed in the synthesis of oligonucleotide models for the so-called RNA X structure. Embedding the inherently unstable trinucleoside phosphotriester as a branching unit within an oligonucleotide structure stabilizes it towards hydrolysis by an order of magnitude. Hybridization of such a branched oligonucleotide with a fully complementary oligonucleotide results in further stabilization, by another order of magnitude. Interestingly, hybridization with oligonucleotides through which the branching phosphotriester linkage is placed in a kinked environment, rather than a double-stranded position, yields structures that are moderately more stable than their fully double-stranded counterparts. The half-life of the most stable of such structures (at 25 °C and pH 7.38) is more than 24 h, whereas under the same conditions the half-life of the trinucleoside phosphotriester branching unit lacking any oligonucleotide arms is only approximately 3 min. When extrapolated to the conditions used for the kinetic analysis of the hydrolysis of RNA X (50 °C and pH 9), the former value is only approximately three times shorter than the corresponding value for RNA X (6 and 20 min, respectively). The proposal that the two oligonucleotide strands of RNA X are connected by a phosphotriester linkage would hence seem plausible in view of the elaborate tertiary structure of this unusual species. On a more general level the results indicate that, suitably folded, phosphate-branched RNA can be surprisingly stable and should not be dismissed outright as an intermediate in biologically relevant phosphate-transfer reactions.

Experimental Section

General: The nucleosides, protected nucleoside phosphoramidites, and other reagents were commercial products that were used as received. NMR spectra were recorded with Bruker Avance 400 or 500 NMR spectrometers and mass spectra with a Bruker MicroTOF-Q high-resolution ESI mass spectrometer. The oligonucleotides were assembled on an Applied Biosystems 3400 DNA synthesizer.

Kinetic measurements: Hydrolytic reactions of the phosphate-branched oligonucleotide **10a** were carried out in sealed tubes immersed in a water bath, the temperature of which was adjusted to (25.0 ± 0.1) °C. Firstly, the starting material and any additional oligonucleotides were dissolved in aq. NaCl (0.10 mol L^{-1}) and allowed to hybridize for 15 min before the start of the reaction. An equal amount of TCEP buffer (100 mM, pH 7.38, $I = 0.22$ mol L^{-1}) was then added to this solution. The initial concentrations of the oligonucleotides were 3.0 μmol L^{-1}. The compositions of samples withdrawn at appropriate time intervals were analyzed by anion-exchange HPLC on a Dionex DNA Swift SAX-1S column (5 × 150 mm, monolithic), with elution with a linear gradient of $NaClO_4$ (0.33 mol L^{-1}, 10→60% over 25 min, flow rate 1.5 mL min^{-1}) in Tris buffer (20 mmol L^{-1}, pH 7.0). The observed retention times (t_R [min]) for the hydrolytic products of **10a** and the complementary oligonucleotides used in this study were as follows: 15.1 (**10c**), 12.1 (**11**), 12.1 (**17b**), 11.0 (**17a**), 10.9 (**13**), 10.5 (**15**), 9.7 (**18a**), 9.6 (**16**), 8.7 (**18b**), 5.5 (**14**), 2.1 (**12**). The products were characterized by spiking with authentic samples and the peak areas were converted to relative concentrations by using molar absorption coefficients calculated by an implementation of the nearest-neighbors method. In each case the ratio of P–O3′ to P–O5′ bond cleavage was obtained as the ratio of the relative concentrations of the corresponding decamer and pentamer oligonucleotide products **14** and **12**.

Under the reducing conditions of the reaction buffer, three consecutive reactions take place. Firstly, the disulfide bond of the 2′-*O*-*tert*-butyldithiomethyl protecting group is broken in a reaction that is too rapid to be followed by HPLC. The hydrolysis of the resulting 2′-thiohemiacetal is a much slower process, with a half-life of approximately 90 min under the experimental conditions. Finally, the free 2′-OH group attacks the phosphorus atom in the scissile phosphotriester linkage, initiating the reaction of interest. With single-stranded **10c**, this reaction is faster than the preceding deprotection step, so the rate law for consecutive first-order reactions had to be applied to obtain the desired pseudo first-order rate constant. In all the other cases the cleavage of **10c** was sufficiently slow that the simple first-order rate law could be used instead. With each system except **10c**:**16**, the pseudo first-order rate constant for the cleavage of **10c** was obtained by applying the appropriate rate law to the time-dependent increase in the relative concentration of the decamer oligonucleotide product **14**. With **10c**:**16**, this product remained hybridized to the complementary oligonucleotide **16**, precluding reliable determination of its concentration. In this case, the rate constant was based on the formation of the pentamer oligonucleotide product **12** instead. From our earlier experience with the reactions of ribonucleoside 3′-phosphotriesters, isomerization of **10c** is in all likelihood a very rapid reaction that reaches equilibrium even before the first sample is withdrawn.[2,4] Because of the similar retention times and the general broadness of the HPLC peaks of all the phosphate-branched oligonucleotide species, this reaction could not be detected. For the

same reasons, the observed rate constants could not be broken down to individual contributions of R_P and S_P diastereomers of **10c**.

3′-*O*-(*tert*-Butyldimethylsilyl)-5′-*O*-levulinoyl-2′-*O*-methyluridine (5): Levulinic acid (4.68 g, 40.30 mmol) and DCC (4.18 g, 20.26 mmol) were dissolved in anhydrous dioxane and the resulting mixture was stirred at room temperature for 2 h, after which it was filtered, and the filtrate was added to a solution of 3′-*O*-(*tert*-butyldimethylsilyl)-2′-*O*-methyluridine (1.91 g, 5.13 mmol) in anhydrous pyridine (20 mL). The reaction mixture was then stirred at room temperature for 16 h, after which it was concentrated to dryness. The residue was dissolved in CH_2Cl_2 (100 mL) and washed with saturated aq. $NaHCO_3$ (100 mL). The aqueous phase was back-extracted with CH_2Cl_2 (100 mL), and the combined organic phases were dried with Na_2SO_4 and concentrated to dryness. The crude product was purified by silica gel chromatography with elution with a mixture of MeOH and CH_2Cl_2 (4:96, *v/v*). Yield: 1.65 g (75%); ^{1}H NMR ($CDCl_3$, 400 MHz): δ = 9.12 (br s, 1H), 7.72 (d, J = 8.2 Hz, 1H), 5.85 (d, J = 2.2 Hz, 1H), 5.78 (d, J = 8.2 Hz, 1H), 4.42 (dd, J_1 = 2.4 Hz, J_2 = 12.6 Hz, 1H), 4.32 (dd, J_1 = 3.2 Hz, J_2 = 12.6 Hz, 1H), 4.20 (m, 1H), 4.15 (dd, J_1 = 5.0 Hz, J_2 = 7.6 Hz, 1H), 3.72 (dd, J_1 = 2.2 Hz, J_2 = 4.8 Hz), 3.56 (s, 3H), 2.81 (ddd, J_1 = 6.2 Hz, J_2 = J_3 = 2.9 Hz, 2H), 2.57 (ddd, J_1 = 6.2 Hz, J_2 = 1.5 Hz, J_3 = 2.1 Hz, 2H), 2.20 (s, 3H), 0.90 (s, 9H), 0.10 (s, 3H), 0.09 ppm (s, 3H); ^{13}C NMR ($CDCl_3$, 100 MHz): δ = 206.2, 172.2, 163.2, 150.0, 139.8, 102.3, 88.7, 83.4, 81.2, 69.6, 62.2, 58.5, 37.8, 30.7, 29.7, 25.6, 18.1, −4.7, −5.1 ppm; HRMS (ESI$^+$): *m/z* calcd: 493.1977 $[M+Na]^+$; found: 493.1952.

5′-*O*-Levulinoyl-2′-*O*-methyluridine (6): Compound **5** (1.65 g, 3.51 mmol) was dissolved in THF (41.25 mL). Triethylamine trihydrofluoride (2.285 mL, 14.02 mmol) was added, and the resulting mixture was stirred at room temperature for 64 h, after which it was concentrated under reduced pressure. The crude product was purified by silica gel chromatography with elution with MeOH/CH_2Cl_2 (3:97, *v/v*). Yield: 1.12 g (89%); ^{1}H NMR ($CDCl_3$, 500 MHz): δ = 8.39 (br s, 1H), 7.73 (d, J = 10.2 Hz, 1H), 5.91 (d, J = 2.5 Hz, 1H), 5.79 (dd, J_1 = 10.3 Hz, J_2 = 2.9 Hz, 1H), 4.46 (br s, 1H), 4.45 (br s, 1H), 4.18 (m, 1H), 4.13 (m, 1H), 3.85 (dd, J_1 = 6.2 Hz, J_2 = 2.6 Hz, 1H), 3.65 (s, 3H), 2.83 (ddd, J_1 = 7.5 Hz, J_2 = 2.8 Hz, J_3 = 1.7 Hz, 2H), 2.72 (d, J = 9.9 Hz, 1H), 2.56 (ddd, J_1 = 8.0 Hz, J_2 = 2.4 Hz, J_3 = 1.5 Hz, 2H), 2.21 ppm (s, 3H); ^{13}C NMR ($CDCl_3$, 125 MHz): δ = 206.6, 172.4, 162.7, 149.8, 139.5, 102.5, 87.8, 83.3, 81.7, 68.6, 62.4, 58.8, 37.9, 29.8, 27.8 ppm; HRMS (ESI$^+$): *m/z* calcd: 379.1112 $[M+Na]^+$; found: 379.1107.

2′-*O*-(*tert*-Butyldithiomethyl)-5′-*O*-(4,4′-dimethoxytrityl)uridin-3′-yl 5′-*O*-levulinoyl-2′-*O*-methyluridin-3′-yl *N*,*N*-diisopropylphosphoramidite (8a): Compound **6** (0.6319 g, 1.773 mmol) was coevaporated from anhydrous pyridine (3×10 mL) and the residue was dissolved in anhydrous CH_2Cl_2. Anhydrous triethylamine (1.2 mL) and *N*,*N*,*N*′,*N*′-tetraisopropylchlorophosphorodiamidite (0.5257 g, 1.970 mmol) were added, and the resulting mixture was stirred at room temperature for 4 h, after which it was diluted with CH_2Cl_2 (100 mL) and washed with saturated aq. $NaHCO_3$ (100 mL). The organic phase was dried with Na_2SO_4 and concentrated to dryness. The residue and 2′-*O*-(*tert*-butyldithiomethyl)-5′-*O*-(4,4′-dimethoxytrityl)uridine[11] (0.6025 g, 0.885 mmol) were dissolved under nitrogen in a solution of 5-benzylthio-1*H*-tetrazole in MeCN (0.25 M, 3.3 mL). The reaction mixture was stirred at room temperature for 3 h, after which it was diluted with CH_2Cl_2 (100 mL) and washed with saturated aq. $NaHCO_3$ (100 mL). The aqueous phase was back-extracted with CH_2Cl_2, and the combined organic phases were dried with Na_2SO_4 and concentrated to dryness. The residue was purified by silica gel chromatography with elution first with Et_3N/EtOAc/CH_2Cl_2 (1:79:20, *v/v/v*) and finally with Et_3N/MeOH/CH_2Cl_2 (1:9:90, *v/v/v*). Yield: 0.2673 g (25%) as a 1:1 mixture of R_P and S_P diastereomers (the absolute configuration at phosphorus was not established). HRMS (ESI$^+$): *m/z* calcd: 1188.4045 $[M+Na]^+$; found: 1188.3976.

Diastereomer A: ^{1}H NMR ($CDCl_3$, 500 MHz): δ = 7.99 (d, J = 8.2 Hz, 1H), 7.55 (d, J = 8.2 Hz, 1H), 7.45–7.21 (m, 9H), 6.85 (m, 4H), 6.11 (d, J = 4.1 Hz, 1H), 5.83 (d, J = 2.4 Hz, 1H), 5.74 (d, J = 8.2 Hz, 1H), 5.26 (d, J = 8.1 Hz, 1H), 5.07 (d, J = 11.2 Hz, 1H), 4.98 (d, J = 11.3 Hz, 1H), 4.81 (ddd, J_1 = 5.0 Hz, J_2 = 4.7 Hz, J_3 = 9.1 Hz, 1H), 4.58 (dd, J_1 = 4.5 Hz, J_2 = 4.6 Hz, 1H), 4.38 (m, 1H), 4.31 (m, 1H), 4.16 (m, 1H), 4.14 (m, 1H), 4.09 (ddd, J_1 = 5.2 Hz, J_2 = 3.4 Hz, J_3 = 8.5 Hz, 1H), 4.01 (dd, J_1 = 2.6 Hz, J_2 = 4.6 Hz, 1H), 3.80 (s, 3H), 3.80 (s, 3H), 3.56 (m, 2H), 3.51 (m, 2H), 3.45 (s, 3H), 2.77 (m, 2H), 2.52 (m, 2H), 2.18 (s, 3H), 1.31 (s, 9H), 1.20 (d, J = 6.6 Hz, 6H), 1.15 ppm (d, J = 6.7 Hz, 6H); ^{13}C NMR ($CDCl_3$, 125 MHz): δ = 206.2, 172.1, 163.7, 163.5, 158.7, 150.3, 150.1, 144.3, 140.5, 139.7, 135.3, 135.0, 130.3, 130.2, 130.2, 128.3, 128.2, 128.1, 128.0, 127.2, 113.4, 113.2, 113.2, 102.4, 102.3, 88.8, 87.0, 83.6, 82.3, 81.2, 80.6, 78.2, 70.4, 68.4, 62.4, 61.7, 58.4, 55.3, 55.2, 47.4, 44.5, 37.7, 29.8, 29.8, 27.7, 24.7, 24.7 ppm; ^{31}P NMR ($CDCl_3$, 202 MHz): δ = 148.9 ppm.

Diastereomer B: ^{1}H NMR ($CDCl_3$, 500 MHz): δ = 7.81 (d, J = 8.2 Hz, 1H), 7.66 (d, J = 8.2 Hz, 1H), 7.45–7.21 (m, 9H), 6.85 (m, 4H), 6.13 (d, J = 6.0 Hz, 1H), 6.02 (d, J = 4.0 Hz, 1H), 5.91 (d, J = 8.2 Hz, 1H), 5.33 (d, J = 8.2 Hz, 1H), 4.96 (m, 2H), 4.61 (dd, J_1 = 5.1 Hz, J_2 = 5.7 Hz), 4.46 (m, 3H), 4.36 (m, 1H), 4.19 (m, 1H), 4.16 (m, 1H), 3.88 (dd, J_1 = 4.5 Hz, J_2 = 4.8 Hz, 1H), 3.81 (s, 3H), 3.80 (s, 3H), 3.56 (m, 2H), 3.51 (s, 3H), 3.49 (m, 1H), 3.39 (m, 1H), 2.72 (m, 2H), 2.61 (m, 2H), 2.18 (s, 3H), 1.29 (s, 9H), 1.15 (d, J = 6.7 Hz, 6H), 1.06 (d, J = 6.7 Hz, 6H); ^{13}C NMR ($CDCl_3$, 125 MHz): δ = 206.5, 172.4, 163.5, 163.4, 158.7, 150.3, 150.2, 144.0, 140.0, 139.9, 135.1, 134.9, 130.3, 130.2, 130.2, 128.3, 128.2, 128.1, 128.0, 127.2, 113.4, 113.2, 113.2, 103.0, 102.7, 87.9, 86.2, 83.9, 82.4, 81.8, 81.5, 79.0, 71.0, 69.5, 63.3, 62.9, 58.4, 55.3, 55.2, 47.7, 46.0, 43.3, 37.8, 29.8, 29.7, 27.9, 24.6, 24.5 ppm; ^{31}P NMR ($CDCl_3$, 202 MHz): δ = 150.1 ppm.

2′-*O*-(*tert*-Butyldimethylsilyl)-5′-*O*-(4,4′-dimethoxytrityl)uridin-3′-yl 5′-*O*-levulinoyl-2′-*O*-methyluridin-3′-yl *N*,*N*-diisopropylphosphoramidite (8b): 5′-*O*-(4,4′-Dimethoxytrityl)-2′-*O*-(*tert*-butyldimethylsilyl)uridine (0.870 g, 1.32 mmol) was dissolved in anhydrous CH_2Cl_2 (10 mL). Anhydrous triethylamine (1.0 mL) and *N*,*N*,*N*′,*N*′-tetraisopropylchlorophosphorodiamidite (0.420 g, 1.57 mmol) were added, and the resulting mixture was stirred at room temperature for 4 h, after which it was diluted with CH_2Cl_2 (100 mL) and washed with saturated aq. $NaHCO_3$ (100 mL). The organic phase was dried with Na_2SO_4 and concentrated to dryness. The residue and 5′-*O*-levulinoyl-2′-*O*-methyluridine (**6**, 0.330 g, 0.926 mmol) were dissolved under nitrogen in anhydrous MeCN (2.0 mL). A solution of 1*H*-tetrazole in MeCN (0.45 M, 2.05 mL, 0.923 mmol) was added, and the resulting mixture was stirred at room temperature for 16 h, after which it was suspended in saturated aq. $NaHCO_3$ (100 mL). The aqueous mixture was extracted with CH_2Cl_2 (2×100 mL), and the organic layer was dried with Na_2SO_4 and concentrated to dryness. The residue was purified by silica gel chromatography with elution first with Et_3N/EtOAc/CH_2Cl_2 (1:79:20, *v/v/v*) and finally with Et_3N/MeOH/CH_2Cl_2 (1:6:93, *v/v/v*). Yield: 0.2866 g (27%) as a 4:1 mixture of R_P and S_P diastereomers (the absolute configuration at phosphorus was not established). HRMS (ESI$^+$): *m/z* calcd: 1168.4686 $[M+Na]^+$; found: 1168.4540.

Major diastereomer: ^{1}H NMR ($CDCl_3$, 500 MHz): δ = 7.68 (d, J = 8.2 Hz, 1H), 7.55 (d, J = 8.2 Hz, 1H), 7.38–7.22 (m, 9H), 6.90 (m, 4H), 5.93 (d, J = 5.2 Hz, 1H), 5.77 (d, J = 4.4 Hz, 1H), 5.69 (d, J = 8.1 Hz,

1H), 5.34 (d, $J=8.1$ Hz, 1H), 4.53 (ddd, $J_1=4.5$ Hz, $J_2=5.4$ Hz, $J_3=10.0$ Hz, 1H), 4.40 (dd, $J_1=J_2=5.0$ Hz, 1H), 4.35 (m, 1H), 4.25 (dd, $J_1=3.3$ Hz, $J_2=12.5$ Hz, 1H), 4.18 (ddd, $J_1=5.3$ Hz, $J_2=5.0$ Hz, $J_3=9.9$ Hz, 1H), 4.11 (dd, $J_1=4.1$ Hz, $J_2=12.4$ Hz, 1H), 3.98 (m, 1H), 3.93 (dd, $J_1=J_2=4.7$ Hz, 1H), 3.79 (s, 3H), 3.78 (s, 3H), 3.61 (m, 1H), 3.52 (dd, $J_1=4.4$ Hz, $J_2=11.0$ Hz, 1H), 3.44 (dd, $J_1=2.2$ Hz, $J_2=10.3$ Hz, 1H), 3.37 (s, 3H), 2.74 (dd, $J_1=6.1$ Hz, $J_2=6.7$ Hz, 2H), 2.56–2.48 (m, 2H), 2.13 (s, 3H), 1.19 (d, $J=6.8$ Hz, 6H), 1.15 (d, $J=6.8$ Hz, 6H), 0.93 (s, 9H), 0.16 (s, 3H), 0.14 ppm (s, 3H); ^{13}C NMR ($CDCl_3$, 125 MHz): $\delta=206.7$, 172.4, 163.0, 162.9, 158.8, 158.7, 150.6, 150.2, 145.1, 140.2, 139.8, 135.5, 135.4, 130.3, 130.1, 128.0, 127.9, 127.0, 113.1, 102.1, 101.9, 88.2, 87.2, 83.5, 81.9, 80.9, 74.9, 73.0, 70.2, 68.4, 63.4, 62.8, 58.0, 54.9, 54.9, 43.1, 37.4, 28.9, 27.6, 25.2, 24.2, 24.1, −5.2, −5.5 ppm; ^{31}P NMR ($CDCl_3$, 202 MHz): $\delta=$ 149.7 ppm.

Minor diastereomer: ^{1}H NMR ($CDCl_3$, 500 MHz): $\delta=7.69$ (d, $J=$ 8.2 Hz, 1H), 7.60 (d, $J=8.2$ Hz, 1H), 7.38–7.22 (m, 9H), 6.90 (m, 4H), 6.01 (d, $J=6.9$ Hz, 1H), 5.98 (d, $J=5.0$ Hz, 1H), 5.82 (d, $J=8.2$ Hz, 1H), 5.50 (d, $J=8.1$ Hz, 1H), 4.51–4.44 (m, 2H), 4.35 (m, 1H), 4.29 (dd, $J_1=4.3$ Hz, $J_2=12.3$ Hz, 1H), 4.26–4.16 (m, 2H), 3.98 (m, 1H), 3.98, (dd, $J_1=J_2=5.0$ Hz, 1H), 3.80 (s, 3H), 3.79 (s, 3H), 3.61 (m, 1H), 3,52–3.46 (m, 1H), 3.45 (s, 3H), 3.40–3.33 (m, 1H), 2.77 (m, 2H), 2.57 (m, 2H), 2.13 (s, 1H), 1.21 (d, $J=6.9$ Hz, 6H), 1.06 (d, $J=$ 6.8 Hz, 6H), 0.91 (s, 9H), 0.15 (s, 3H), 0.10 ppm (s, 3H); ^{13}C NMR: reliable assignment of this spectrum was not possible owing to the small amount of the minor isomer; ^{31}P NMR ($CDCl_3$, 202 MHz): $\delta=$ 149.4 ppm;

Synthesis of the phosphate-branched oligonucleotide 10a: The branching phosphoramidite building block **8a** (20 mg, 17 μmol) and the CPG-supported pentamer oligonucleotide with a free 5′-OH terminus (1 μmol, loading = 37 μmol g^{-1}) were dissolved in an anhydrous solution of 5-benzylthio-1*H*-tetrazole in MeCN (0.25 mol L^{-1}, 200 μL, 50 μmol). The resulting mixture was shaken for 50 min, after which the support was transferred to an oligonucleotide synthesizer column and washed with MeCN. The support-bound oligonucleotide was then capped by conventional Ac_2O treatment, washed with MeCN, oxidized by the conventional I_2/H_2O treatment, and washed again with MeCN. Assembly of the main chain was completed on an oligonucleotide synthesizer by the standard phosphoramidite strategy for RNA (600 s coupling time) and the 5′-OH terminus was capped by conventional Ac_2O treatment. For elongation of the branching chain, the 5′-*O*-levulinoyl protecting group was first removed by treating the support-bound oligonucleotide with a mixture of hydrazine hydrate, pyridine, and acetic acid (1:32:8, *v/v*) for 30 min. The support was then washed with pyridine, MeOH, CH_2Cl_2, and Et_2O, and assembly of the branching chain was completed on an oligonucleotide synthesizer by the standard phosphoramidite strategy for RNA. The oligonucleotide was released from the support, and the nucleobase and phosphate protecting groups were removed by treating the support with aq. $MeNH_2$ (40%) at room temperature for 90 min. The crude product was purified by anion-exchange HPLC on a Dionex DNA Swift SAX-1S column (5×150 mm, monolithic), with elution with a linear gradient of $NaClO_4$ (0.33 mol L^{-1}, 10→60% in 25 min, flow rate = 1.5 mL min^{-1}) in Tris buffer (pH 7.0, 20 mmol L^{-1}). Finally, the purified product was desalted by RP HPLC on a Thermo ODS Hypersil column (4.6×250 mm, 5 μm) with elution with a linear gradient of MeCN in water (0→70% in 15 min, flow rate = 1.0 mL min^{-1}). An HPLC trace of the crude product mixture is included in the Supporting Information. HRMS (ESI$^-$): *m/z* calcd: 1010.1836 $[M-10H]^{10-}$; found: 1010.1830.

Synthesis of the reference oligonucleotide 11 incorporating a 3′,3′-phosphodiester linkage: The branching phosphoramidite building block **8b** (20 mg, 17 μmol) and CPG-supported 2-(2-hydroxyethylsulfonyl)ethyl succinate linker with a free OH terminus (1 μmol, loading = 38 μmol g^{-1}) were dissolved in an anhydrous solution of 5-benzylthio-1*H*-tetrazole in MeCN (0.25 mol L^{-1}, 200 μL, 50 μmol). The resulting mixture was shaken for 50 min, after which the support was transferred to an oligonucleotide synthesizer column and washed with MeCN. The support-bound oligonucleotide was then capped by conventional Ac_2O treatment, washed with MeCN, oxidized by conventional I_2/H_2O treatment, and washed again with MeCN. Assembly of the longer 3′→5′ strand was completed on an oligonucleotide synthesizer by the standard phosphoramidite strategy for RNA (600 s coupling time) and the 5′-OH terminus was capped by conventional Ac_2O treatment. For elongation of the shorter 3′→5′ strand, the 5′-*O*-levulinoyl protection was first removed by treating the support-bound oligonucleotide with hydrazine hydrate/pyridine/acetic acid (1:32:8, *v/v/v*) for 30 min. The support was then washed with pyridine, MeOH, CH_2Cl_2, and Et_2O, and assembly of the shorter strand was completed on an oligonucleotide synthesizer by the standard phosphoramidite strategy for RNA. The oligonucleotide was released from the support, and the nucleobase and phosphate protecting groups were removed by treating the support with aq. $MeNH_2$ (40%) for 90 min at room temperature. The single 2′-*O*-TBDMS protection was removed by conventional $Et_3N{\cdot}3HF$ treatment and the crude product was purified first with a Glen Research Poly-Pak II RP cartridge, followed by anion-exchange HPLC on a Dionex DNA Swift SAX-1S column (5×150 mm, monolithic), with elution with a linear gradient of $NaClO_4$ (0.33 mol L^{-1}, 10→100% in 30 min, flow rate = 1.5 mL min^{-1}) in Tris buffer (pH 7.0, 20 mmol L^{-1}). Finally, the purified product was desalted by RP HPLC on a Thermo ODS Hypersil column (4.6×250 mm, 5 μm) with elution with a linear gradient of MeCN in water (0→70% in 15 min, flow rate = 1.0 mL min^{-1}). An HPLC trace of the crude product mixture is included in the Supporting Information. HRMS (ESI$^-$): *m/z* calcd: 834.6485 $[M-10H]^{10-}$; found: 834.8467.

Acknowledgements

The technical assistance of Kiira Rimpilä in the synthesis of the protected nucleosides is gratefully acknowledged.

Keywords: branched RNA · hydrolysis · mRNA splicing · phosphotriesters · RNA structures · RNA X

[1] a) Z. Zhou, L. J. Licklider, S. P. Gygi, R. Reed, *Nature* **2002**, *419*, 182–185; b) C. L. Will, R. Lührmann, *Cold Spring Harbor Perspectives in Biology*, Cold Spring Harbor Laboratory Press, New York, **2010**; c) J. Rappsilber, U. Ryder, A. I. Lamond, M. Mann, *Genome Res.* **2002**, *12*, 1231–1245; d) C. B. Burge, T. H. Tuschl, P. A. Sharp in *RNA World II* (Eds.: R. F. Gesteland, T. R. Cech, J. F. Atkins), Cold Spring Harbor Laboratory Press, New York, **1998**, pp. 525–560.

[2] M. Kosonen, R. Seppänen, O. Wichmann, H. Lönnberg, *J. Chem. Soc. Perkin Trans. 2* **1999**, 2433–2439.

[3] S. Mikkola, M. Kosonen, H. Lönnberg, *Curr. Org. Chem.* **2002**, *6*, 523–538.

[4] T. Lönnberg, J. Kiiski, S. Mikkola, *Org. Biomol. Chem.* **2005**, *3*, 1089–1096.

[5] B. Singer, L. Sun, H. Fraenkel-Conrat, *Proc. Natl. Acad. Sci. USA* **1975**, *72*, 2232–2236.

[6] T. Lönnberg, *Nucleosides Nucleotides Nucleic Acids* **2006**, *25*, 315–323.

[7] S. Valadkhan, A. Mohammadi, C. Wachtel, J. L. Manley, *RNA* **2007**, *13*, 2300 – 2311.
[8] S. Valadkhan, J. L. Manley, *Nature* **2001**, *413*, 701 – 707.
[9] S. Valadkhan, J. L. Manley, *RNA* **2003**, *9*, 892 – 904.
[10] T. Lönnberg, K.-M. Kero, *Org. Biomol. Chem.* **2012**, *10*, 569 – 574.
[11] A. Semenyuk, A. Földesi, T. Johansson, C. Estmer-Nilsson, P. Blomgren, M. Brännvall, L. A. Kirsebom, M. Kwiatkowski, *J. Am. Chem. Soc.* **2006**, *128*, 12356 – 12357.
[12] T. Horn, M. S. Urdea, *Tetrahedron Lett.* **1986**, *27*, 4705 – 4708.
[13] T. Lönnberg, J. Korhonen, *J. Am. Chem. Soc.* **2005**, *127*, 7752 – 7758.
[14] D. A. Usher, A. H. McHale, *Proc. Natl. Acad. Sci. USA* **1976**, *73*, 1149 – 1153.
[15] a) P. Järvinen, M. Oivanen, H. Lönnberg, *J. Org. Chem.* **1991**, *56*, 5396 – 5401; b) K. Kawamura, *Biochim. Biophys. Acta Gen. Subj.* **2003**, *1620*, 199 – 210.
[16] S. Kuusela, H. Lönnberg, *J. Chem. Soc. Perkin Trans. 2* **1994**, 2109 – 2113.
[17] D. J. Klein, T. M. Schmeing, P. B. Moore, T. A. Steitz, *EMBO J.* **2001**, *20*, 4214 – 4221.
[18] B. Schneider, Z. Morávek, H. M. Berman, *Nucleic Acids Res.* **2004**, *32*, 1666 – 1677.
[19] a) N. Toor, K. S. Keating, S. D. Taylor, A. M. Pyle, *Science* **2008**, *320*, 77 – 82; b) N. Toor, K. Rajashankar, K. S. Keating, A. M. Pyle, *Nat. Struct. Mol. Biol.* **2008**, *15*, 1221 – 1222; c) N. Toor, K. S. Keating, O. Fedorova, K. Rajashankar, J. M. Wang, A. M. Pyle, *RNA* **2010**, *16*, 57 – 69; d) A. M. Pyle, *Crit. Rev. Biochem. Mol. Biol.* **2010**, *45*, 215 – 232.
[20] P. M. Gordon, E. J. Sontheimer, J. A. Piccirilli, *RNA* **2000**, *6*, 199 – 205.
[21] a) T. Lönnberg, *Chem. Eur. J.* **2011**, *17*, 7140 – 7153; b) C. L. Peebles, P. S. Perlman, K. L. Mecklenburg, M. L. Petrillo, J. H. Tabor, K. A. Jarrell, H. L. Cheng, *Cell* **1986**, *44*, 213 – 223; c) R. van der Veen, A. C. Arnberg, G. van der Horst, L. Bonen, H. F. Tabak, L. A. Grivell, *Cell* **1986**, *44*, 225 – 234; d) C. Schmelzer, R. J. Schweyen, *Cell* **1986**, *46*, 557 – 565.

Received: October 1, 2012
Published online on November 26, 2012

